Removal of Potassium Negative Resistance in Perfused Squid Giant Axons

HAROLD LECAR, GERALD EHRENSTEIN, LEONARD BINSTOCK, and ROBERT E. TAYLOR

From the National Institutes of Health, Bethesda, Maryland, and the Marine Biological Laboratory, Woods Hole, Massachusetts

ABSTRACT Squid giant axons, internally and externally perfused with solutions having potassium as the only cation, exhibit an approximately linear steady-state current-voltage relation. When small amounts of calcium and magnesium are present in the external potassium solution, the current-voltage curve is markedly nonlinear, exhibiting the rectification and negative resistance which have been observed for intact axons in isosmotic potassium solutions. The effects of perfusion and removal of external divalent cations are interpreted in terms of two components of current, a linear component and a nonlinear time-varying component. The former is increased and the latter diminished by the removal of the external divalent cations.

INTRODUCTION

Squid giant axons bathed in solutions having high potassium concentration exhibit a negative resistance steady-state current-voltage curve (1, 2) which gives rise to an anodal jump phenomenon (3). Such steady-state negative resistance characteristics have been observed in a number of other preparations (4–8). In contrast to the negative resistance seen for intact axons of the North Atlantic squid, *Loligo pealii*, a linear steady-state current-voltage relation has been found for internally perfused axons of the Chilean squid, *Docidicus gigas* (9). In both these experiments the axons were bathed in Ca^{++}- and Mg^{++}-free KCl solutions, and aside from possible species variations, the only difference in experimental conditions was the perfusion. This suggests that the internal perfusion removes or alters some constituent of the axoplasm necessary for the negative resistance. Such a result means that the negative resistance is not an intrinsic property of the axon membrane, independent of the environment. In order to verify this conclusion, we measured voltage-clamp currents for perfused axons of *Loligo pealii*. This was done to eliminate the possibility that the difference in current-voltage curves is merely due to the difference in species.

The seeming effect of perfusion in changing the nonlinear current-voltage curve into one which is essentially linear is analogous to the change in rectification of intact axons in artificial seawater caused by changes in external calcium concentration (10). Numerous other effects of calcium on the electrical properties of axons have also been studied (11). One purpose of our experiment was to determine whether the nonlinearities can be restored to a perfused axon by the addition of external calcium. In addition, we studied the transient approach to the steady state, in order to compare the currents in isosmotic potassium with those observed for intact squid axons.

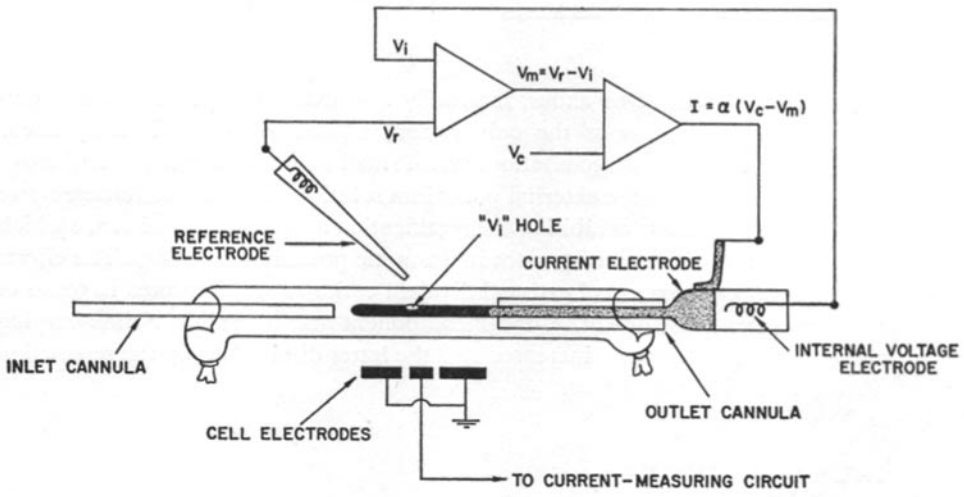

FIGURE 1. Schematic diagram of the voltage-clamp perfusion apparatus.

METHODS

Experiments were performed on giant axons of the squid *Loligo pealii*. Tied off lengths of axon, about 5 cm, were dissected from the mantles of freshly killed squid under flowing seawater. The axons were then cleaned of surrounding tissue, but a layer of fibrous tissue about 50 μ thick was always left. This layer was found necessary for maintaining the mechanical strength of the preparation during the perfusion. The main purpose of the cleaning was to render the axon transparent so that the internal electrodes and perfusion pipettes could be seen. Axon diameters varied from 400 to 500 μ.

The axon chambers and various cannulae were essentially scaled-down counterparts of the apparatus used by Rojas and Ehrenstein (9), for voltage-clamp experiments on the larger perfused axons (700–1000 μ) of the Chilean squid, *Docidicus gigas*. The placement of the perfusion pipettes and the electrodes is indicated schematically in Fig. 1. Axons were mounted horizontally in the chamber and bathed in cold flowing external solutions. The external solutions used were: artificial seawater (430 mM Na^+, 10 mM K^+, 10 mM Ca^{++}, 50 mM Mg^{++}, 560 mM Cl^-, and 5 mM tris (hydroxymethyl) aminomethane (Tris), used to buffer the solution to a pH of 7.4 ± 0.1), high potassium solu-

tion (500 mM KCl or KF, and Tris at pH 7.4), and high potassium solution with restored divalent cations (440 mM K^+, 10 mM Ca^{++}, 50 mM Mg^{++}, 560 mM Cl^-, and Tris at pH 7.4).

The perfusion technique was based on the method of Tasaki and coworkers (12–14). It consists of two steps, first sucking out the axoplasm through a 300 μ diameter pipette inserted into a cut in one end of the axon, and then introducing the perfusion fluid from the other end of the axon through a 150 μ pipette inserted into another cut. Both pipettes are mounted on micromanipulators, and are manipulated so that after some axoplasm has been sucked out, the smaller pipette is moved coaxially down the axon and into the suction pipette, which is now used as a solution outlet. While the perfusion fluid is flowing and washing out some residual axoplasm, the two pipettes are separated, leaving a perfused region about 15 mm in length.

The voltage-clamp technique and the necessary feedback circuits have been described by Moore and Cole (15). The voltage drop across the membrane is maintained by an electronic feedback circuit which compares the measured membrane voltage, V_m, to a command voltage, V_c. The difference, $V_c - V_m$, is fed to an operational amplifier used to supply current radially along a length of the perfused region. The currents needed to maintain a given step potential are recorded as a function of time.

The axial electrode shown in Fig. 1 is a combination current-supplying and voltage-measuring electrode, and is a modification by Binstock of the coaxial voltage-clamp electrodes developed by Armstrong and Binstock (16). The combination electrode consists of a glass capillary 100 μ in diameter which is coated on the outside with silver print, over which silver is deposited electrolytically, and then plated with platinum black. This platinum electrode is the current-supplying electrode, which sends radial currents to the platinum cell electrodes. The current is measured through the central cell electrode; the outer cell electrodes are grounded and serve as guards to minimize fringe effects in the measuring region.

The combination electrode has a hole, 25 μ in diameter, 7.5 mm from its end. This is the voltage-measuring point of the point-control voltage-clamp system. The electrode is filled with 0.5 M KCl. It has a thin platinum wire in the 100 μ region for reducing high frequency impedance and a Ag-AgCl wire in the shank. The membrane voltage, V_m, is measured between this electrode and an external reference pipette filled with agar–0.5 M KCl and having a Ag-AgCl reference.

The combination electrode is convenient for voltage-clamp perfusion experiments on small axons. It eliminates the need for two separate internal electrodes, which would be difficult to fit into axons less than 500 μ in diameter. Unfortunately, voltage-clamp currents measured with this system tend to show a marked decay at times of the order of 10–100 msec. The probable cause for this decay is that polarization currents near the control point cause the membrane voltage to drift slowly to a value lower than the command voltage. This effect is similar to what would happen if the control point and the current electrode were coupled electrically. The current records are similar to those obtained in the first voltage-clamp experiments (17), in which the current electrode itself was used as the voltage electrode.

To ascertain that the decay was in fact a result of the method of voltage control, we did experiments on unperfused axons in which the coaxial electrode was used in conjunction with a microtip, and the axon was clamped alternately using one type

of control or the other. The experiments showed that the current records were identical except for the slow falloff.

The polarization artifact described above can cause uncertainty in the value of the steady-state current, and consequently must be corrected for. It was noticed that the

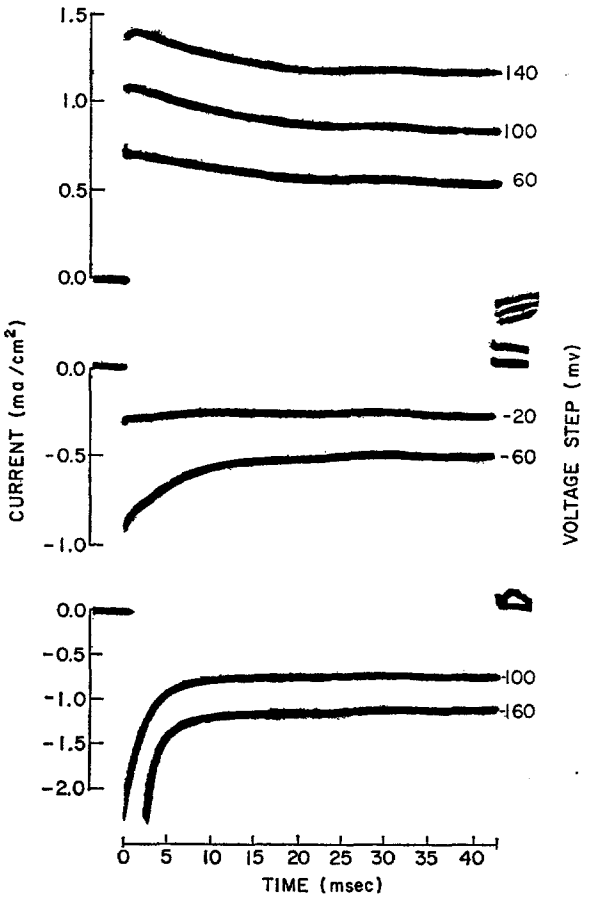

FIGURE 2. Composite photograph of oscilloscope traces of membrane currents for depolarizing (+) and hyperpolarizing (−) steps; internal solution 500 mM KF, external solution 500 mM KCl, temperature 12.5°C. The small turn-on transient is seen in the early part of the $V = +140$ mv record. Axon 65B30.

polarizing electrode produces an undershoot of current at the end of the clamp pulse (Fig. 2). This undershoot occurs because the membrane voltage does not return to zero when the pulse is shut off, but instead switches back to a voltage displaced by the electrode polarization. From the measured instantaneous current-voltage curve, the voltage corresponding to a particular current undershoot was determined. This voltage was then subtracted from the nominal command voltage to determine the corrected voltage corresponding to the end point on the record. Experimental instantane-

ous current-voltage curves used for this correction are shown in Fig. 5, where they are seen to be linear in the voltage range −100 mv to +100 mv. Fig. 3 shows both the corrected and uncorrected steady-state current-voltage curves for one axon. In this case, the correction is not very large. In the worst case, the correction was about

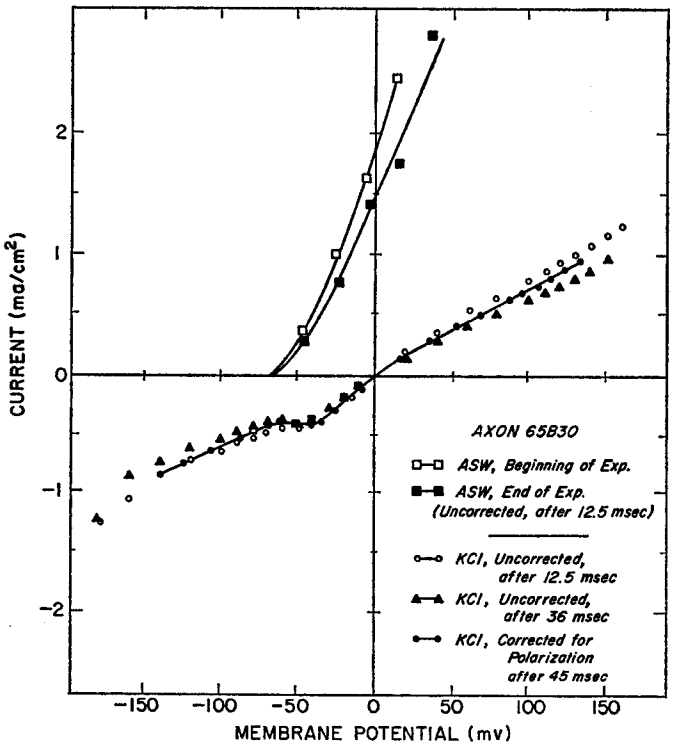

FIGURE 3. Steady-state current-voltage curves, internal solution 500 mM KF. Open squares, external ASW, beginning of experiment, uncorrected data, 12.5 msec after initiation of the voltage step. Filled squares, external ASW, end of experiment, uncorrected data after 12.5 msec. Open circles, external 500 mM KCl, uncorrected data, after 12.5 msec. Filled triangles, external 500 mM KCl, uncorrected data, after 36 msec. Filled circles, external 500 mM KCl, corrected for electrode polarization, after 45 msec. Voltages are given relative to the resting potential in external KCl. Axon 65B30. V_{rest} = +15 mv. Temperature, 12.5°C.

1.5 times as great, but in no case did the correction change the qualitative appearance of the curve. Corrected steady-state current-voltage curves for a number of axons are shown in Fig. 4.

Membrane potential values shown in this paper are taken relative to the measured resting potential of the axon in isosmotic potassium. Generally the resting potential was within a few millivolts of zero (the potassium equilibrium potential). There was no obvious correlation between small departures from zero and the anion composition, but resting potentials were not studied systematically. In Figs. 3, 8, and 10

where curves for two different external potassium concentrations are shown, the zero of potential is the resting potential in isosmotic potassium and the origin of the ASW curves is shifted by appropriate amounts.

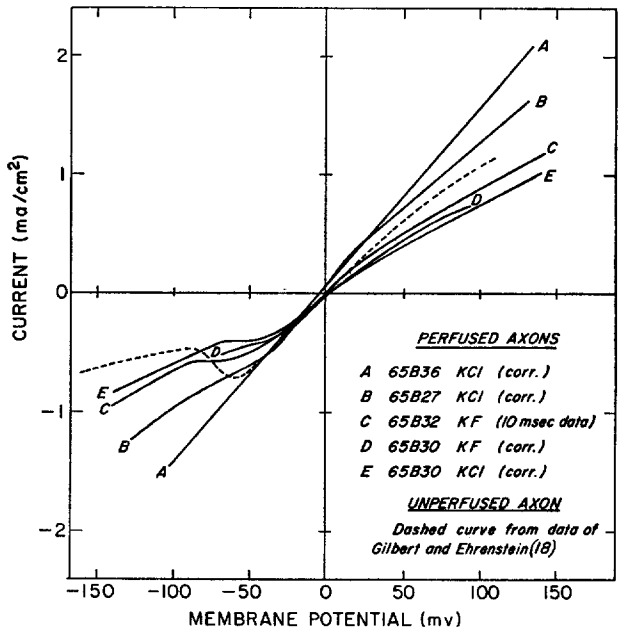

FIGURE 4. Corrected steady-state current-voltage curves for axons internally perfused with 500 mM KF.

Curve	*Axon*	*External solution*
A	65B36	500 mM KCl
B	65B27	500 mM KCl
C	65B32	500 mM KF
D	65B30	500 mM KF
E	65B30	500 mM KCl

Dashed curve shows the corresponding current-voltage curve for an intact axon in external isosmotic KCl, taken from the data of Gilbert and Ehrenstein (18).

RESULTS

A typical experiment consists of a voltage-clamp control run on an axon internally perfused with 500 mM KF and externally bathed in cooled, flowing artificial seawater (ASW), a voltage-clamp run with a high potassium external solution, and finally another control in external ASW. The control runs give the well known response expected for intact axons in ASW with no significant changes caused by the internal perfusion. Fig. 2 shows a set of current responses to various voltage-clamp step voltages with an external solution containing 500 mM KCl. The records show a fast initial surge of current followed by a transient rise or fall to the steady-state value. In most of the

records the "steady-state" current does not persist, but decays with a relatively long time constant. This decay was shown to be an artifact of the coaxial electrode system and must be corrected for in the manner we have described in order to obtain accurate steady-state values.

The current measured 200 μsec after the voltage-clamp pulse is turned on is

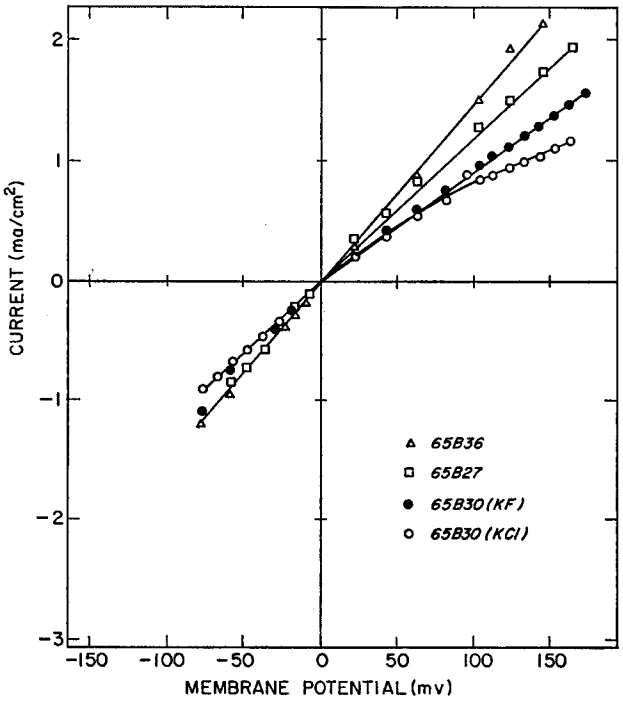

FIGURE 5. Initial current-voltage curves; current measured 0.2 msec after initiation of voltage step.

	Axon	*External solution*
△—△—△	65B36	500 mM KCl
□—□—□	65B27	500 mM KCl
●—●—●	65B30	500 mM KF
○—○—○	65B30	500 mM KCl

called the initial current. This time is shorter than any of the relevant membrane transients, but longer than the capacitative time constant of the voltage-clamp system. Initial current as a function of membrane potential is shown in Fig. 5 for several axons. The average initial conductance is approximately 14 mmho/cm².

After the initial burst of current, there is a transient decay or rise to a steady state with a time constant of a few milliseconds. Both uncorrected and corrected steady-state current-voltage curves for one axon are shown in Fig. 3. The currents for a comparison run in ASW are also shown and have the typi-

cal ASW steady-state shape. Fig. 4 shows the corrected steady-state current-voltage curves for several axons. The typical curve is seen to be approximately linear but with a slight rectification and a discernable bump or transition region centered about $V \cong -50$ mv. This pattern is characteristic of all the axons measured although the extent of the rectification and the relative height of the bump vary somewhat from axon to axon. Fig. 4 shows axons covering the extreme range of this effect.

Fig. 6 demonstrates the influence on the shape of the current-voltage curve

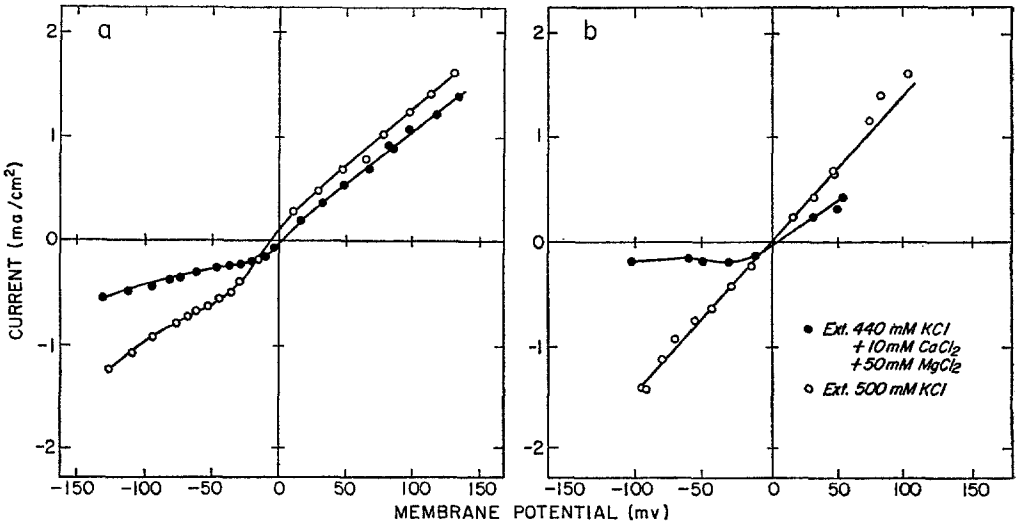

FIGURE 6. Effect of external calcium-magnesium on steady-state current-voltage curve of a perfused axon. Open circles, external solution: 500 mM KCl. Filled circles, external solution: 440 mM KCl + 10 mM $CaCl_2$ + 50 mM $MgCl_2$. (*a*) Effect of calcium-magnesium restoration. Initial run in external KCl. Axon 65B27. (*b*) Effect of calcium-magnesium removal. Initial run in KCl with $CaCl_2$ and $MgCl_2$. Axon 65B36.

of 10 mM Ca^{++} plus 50 mM Mg^{++} added externally. Fig. 6 *a* shows that this addition increases the rectification markedly for a perfused axon which had previously shown a linear current-voltage curve. Fig. 6 *b* shows the effect of removal of the calcium-magnesium mixture, a nonlinear (rectifying, negative resistance) curve is transformed into a linear characteristic. Thus the effect of adding or removing these divalent cations is at least partly reversible.

The effects of the external anions used are indicated in Fig. 4, where it can be seen that the current-voltage curves are virtually unaltered by the replacement of external chloride solutions with equivalent fluoride solutions. A single experiment was performed to test the effect of internal sodium ions (perfusing solution: 450 mM KF, 50 mM NaF); the current-voltage curve, not shown here, was typical of the nearly linear family of Fig. 4, showing that the restoration

of internal Na^+ has little or no influence on the shape of the current-voltage curve.

Small residual nonlinearities are seen for most of the perfused axons. The limiting currents for both large depolarizing and large hyperpolarizing voltages are linear. These facts suggest that the currents may be decomposed into two components, a linear component and a component with a voltage-dependent conductance which varies sharply in the region between about −40 and −60 mv.

Thus, the steady-state current may be represented by the formula

$$I = [g_o + g_1 f(V)]V \qquad (1)$$

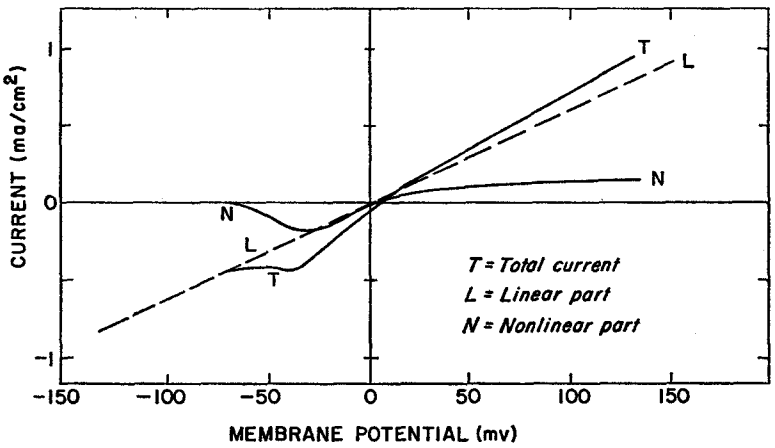

FIGURE 7. Separation of experimental steady-state current into two components; T = total current, L = linear component, and N = nonlinear component. Axon 65B30.

where g_o is the limiting slope of the current in the extreme hyperpolarizing region, g_1 is the slope of the additional current in excess of g_oV in the extreme depolarizing region (i.e., the sum, $g_o + g_1$, is equal to the asymptotic slope for large positive voltages), and V is the membrane voltage. The separation into two components of current is shown in Fig. 7. Each value of the nonlinear component of current shown in Fig. 7 is divided by the corresponding voltage in order to obtain a steady-state voltage-dependent conductance. This conductance, divided by g_1, is the function $f(V)$, and is plotted in Fig. 8 as a function of membrane voltage. Here $f(V)$ is a dimensionless function describing the transition region and ranging from 0 to 1. Values of g_o, g_1, the rectification ratio, and $V_{1/2}$, the value of voltage for which $f(V) = \frac{1}{2}$, are presented in Table I.

Another characteristic parameter that can be determined from these experiments is the rate constant for the approach to steady state. Fig. 2 shows

that for hyperpolarizing voltages there is a clear decrease in membrane current from the initial value. For depolarizing pulses, the current records are relatively flat, but for higher voltages they show a small increase in membrane current at early times. The rising transients in these records are too small to be measured accurately, and the following analysis is limited to the hyperpolarizing transients.

Fig. 9 shows the transient decay on a semilogarithmic plot for some of the voltage-clamp records. It can be seen that the transients are fit reasonably well by single exponentials, and that the rate constants are voltage-dependent.

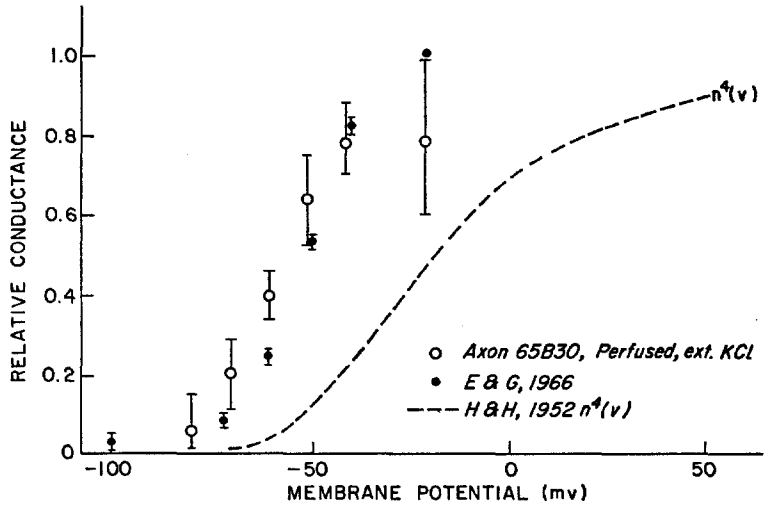

FIGURE 8. Relative steady-state conductance vs. membrane potential. Open circles, axon 65B30; internal KF (perfused), external KCl. Closed circle, Ehrenstein and Gilbert (2); internal axoplasm (unperfused); external KCl (10 mM Ca, 50 mM Mg also present). Dashed line, $n^4(V)$ based on work of Hodgkin and Huxley (19); internal axoplasm (unperfused), external seawater.

Fig. 10 shows the rate constant plotted as a function of voltage. The errors shown are primarily caused by the polarization artifact, which makes the choice of asymptote for this log plot somewhat ambiguous.

DISCUSSION

Fig. 4 shows a striking difference between the steady-state current-voltage curve for perfused and unperfused axons of *Loligo pealii* in isosmotic potassium solution. The curves are approximately linear for perfused axons, but have pronounced negative resistance regions for unperfused axons (1, 2).

Internal perfusion with 500 mM KF does not significantly alter the internal potassium concentration, but the perfusion fluid does wash out other constituents of axoplasm, other ions, neuroproteins, mitochondria, etc. Thus, we con-

clude that, in the absence of external divalent cations, at least one of these axoplasm constituents is necessary for the potassium voltage-dependent conductance.

The linear character of the steady-state current-voltage curve for the perfused axon has already been demonstrated by Rojas and Ehrenstein (9) for

TABLE I

STEADY-STATE CONDUCTANCE

Axon	External solution*	g_o	g_1	Rectification ratio $(g_o+g_1)/g_o$	$V_{1/2}$	ASW‡ leakage g_L
		mmho/cm²	*mmho/cm²*		*mv*	*mmho/cm²*
		Perfused axons, no external calcium				
A. B36	0.5 M KCl	15.5	0.3	1.0	—	5.1
B. B27	0.5 M KCl	9.9	2.8	1.3	−66	9.3
C. B32	0.5 M KF	6.8	2.5	1.4	—	7.6
D. B30	0.5 M KF	9.0	1.3	1.2	−57	10.4
E. B30	0.5 M KCl	6.1	1.2	1.2	−61	6.3
F. B34	0.5 M KCl§	7.3	2.2	1.3	—	—
G. B16	0.5 M KCl‖	6.0	3.0	1.5	—	—
H. B16	0.5 M KF‖	6.0	3.0	1.6	—	—
		Perfused axons, calcium added externally				
I. B27	0.44 M KCl 0.01 M $CaCl_2$ 0.05 M $MgCl_2$	4.6	5.5	2.2	−37	9.3
J. B36	0.44 M KCl 0.01 M $CaCl_2$ 0.05 M $MgCl_2$	1.8	6.4	4.6	−48	2.4
		Unperfused axons				
K.	0.5 M KCl¶	4.2	9.5	3.3	−68	5.0
L.	0.44 M KCl¶ 0.01 M $CaCl_2$¶ 0.05 M $MgCl_2$	1.7	9.4	6.7	−54	2.0

* Internal solution of perfused axons is 0.5 M KF.

‡ In each case the ASW leakage values refer to the control run after an isosmotic potassium run, except for line J where the ASW value was measured before the isosmotic run.

§ Internal solution, 0.45 M KF, 0.05 M NaF, uncorrected data.

‖ Cysteine added to internal solution, uncorrected data.

¶ Data of Gilbert and Ehrenstein (18).

axons of the Chilean squid, *Dosidicus gigas*. However, the absence of data on unperfused axons of this species in isosmotic potassium led these authors to mention the possibility that the difference in current-voltage curves might be caused by a species difference rather than by the perfusion. The present experiment shows that the change in shape is indeed a result of the perfusion.

Fig. 6 *b* shows that, with 10 mM Ca^{++} and 50 mM Mg^{++} in the external solution, the steady-state current-voltage curve for a perfused axon has a

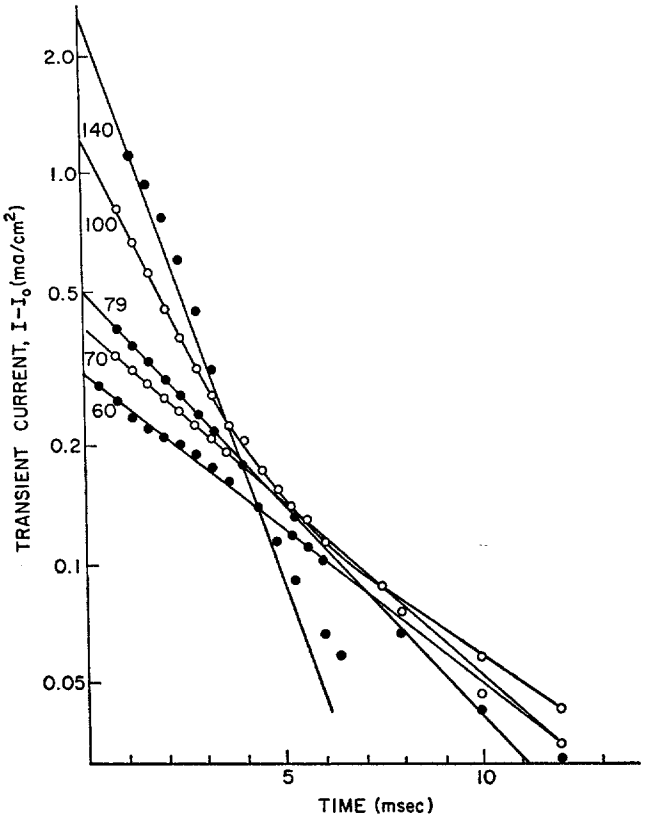

FIGURE 9. Semilogarithmic plot of decay of transient current during hyperpolarizing pulses of various voltages. I is the measured current and I_o is the steady-state current.

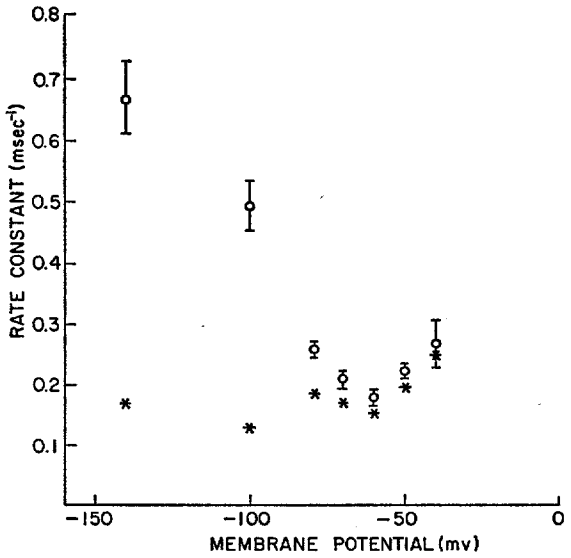

FIGURE 10. Rate constant for change of membrane conductance as a function of membrane voltage. Open circles, raw data. Asterisks, rates inferred for "n^4" process as described in the text.

negative resistance region. This curve is similar to the corresponding current-voltage curve for an unperfused axon in isosmotic potassium (2). However, unperfused axons show no substantial change in the shape of their steady-state current-voltage curves when the external Ca^{++} concentration is varied (18). The curve for the unperfused axon retains its negative-resistance, rectifying shape even with no external calcium. The shape of the steady-state current-voltage curve for a *Loligo pealii* axon in external isosmotic potassium can be described as follows:—

	Perfusion	No perfusion
External Ca^{++}, Mg^{++}	Negative resistance	Negative resistance
No external Ca^{++}, Mg^{++}	Linear	Negative resistance

This tabulation shows that the negative resistance is not an intrinsic property of the membrane alone. In order to eliminate the negative resistance, it is necessary to eliminate calcium and/or magnesium from the outside and some substance from the inside.

In the above tabulation, the designation "linear" is imprecise. Although all the curves for these conditions are far more linear than for the other conditions listed in the tabulation, there is a range of shapes. As shown in Fig. 4, some of the current-voltage curves are completely linear, but some exhibit slight rectification and noticeable bumps on the hyperpolarizing side. The same kind of variability was reported in reference 9. Since some of the axons exhibited complete linearity, it is likely that the residual nonlinearities are due to incomplete perfusion. In any event, these small bumps are in the same voltage range as the negative resistance regions for the other cases in the above tabulation, and it is reasonable to suppose that they all represent the same process. We next inquire what this process is.

In Fig. 7, the current has been separated into two components, one of which is linear with conductance g_o. The remaining component exhibits the same sort of voltage-dependent conductance as is seen for the potassium current of an axon in ASW. The ionic currents of an axon in ASW are described by the Hodgkin-Huxley equations (19). The relevant solution of these equations for the potassium current at a time t after the onset of a voltage-clamp step voltage is:

$$I_K = g_K(V_1 - V_K)[n(V_o) \exp [-t/\tau_n(V_1)] + n(V_1)(1 - \exp [-t/\tau_n(V_1)]]^4 \quad (2)$$

where g_K is a constant with the dimensions of conductance,

V_o is the voltage across the membrane before the voltage-clamp step,

V_1 is the voltage across the membrane during the voltage-clamp step,
V_K is the potassium equilibrium potential given by the Nernst relation,
$n(V)$ and $\tau_n(V)$ are empirical functions of voltage which describe the voltage-dependent conductance and voltage-dependent transient time constant respectively.

The steady-state current ($t \rightarrow \infty$ in equation 2) is

$$I_{ss} = g_K(V_1 - V_K)n^4(V_1). \quad (3)$$

The function $n^4(V)$ as determined from the theory of Hodgkin and Huxley is plotted as the dashed curve in Fig. 8. It is similar in shape to the normalized curve $f(V)$ describing the nonlinear process in isosmotic potassium, although the two curves are displaced from each other by about 30 mv. This suggests that the nonlinear process is the same as the $n(V)$ process in ASW.

A further check on whether the voltage-dependent component of current is similar to that described by Hodgkin and Huxley was made by comparing the rate constants to reach steady-state as a function of voltage. Fig. 10 shows rate constant as a function of voltage for an axon which has a polarization artifact sufficiently small in amplitude and long in duration to allow fairly accurate determination of the true rate constants. This graph shows the rate constants in the hyperpolarizing region. A similar graph for ASW is shown in reference 20. However, the two graphs are not strictly comparable. The ASW data were taken for repolarizations of an axon from a depolarized command voltage back to some hyperpolarized voltage for which $n(V_1) \cong 0$. When $n(V_1) = 0$, equation (2) reduces to:

$$I = g_K(V_1 - V_K)n^4(V_o) \exp [-4t/\tau_n(V_1)], \quad (4)$$

a single exponential whose rate constant is $\lambda_{HH} = 4/\tau_n(V_1)$. In our case the $n(V)$ curve appears to be shifted over by 30 mv, so that at voltages near the ASW resting potential, $n(V_1) \cong 0.5$, and the transient ought to be described as the polynomial of exponentials given by equation (2). By theoretically determining the best single exponential to fit this polynomial and comparing with our experimentally determined single exponentials, we can obtain corrected rate constants which are comparable to those for ASW. This procedure is equivalent to the more tedious process of fitting equation (2) directly to the data, because the experimental points are virtually linear on a semilog plot, as shown in Fig. 9. The corrected rate constants are shown as the stars in Fig. 10. A detailed comparison of the shapes of our curve and the ASW curve is not possible because of the crudeness of this correction. However, for sufficiently large hyperpolarizing voltages, $n(V_1)$ is approximately zero for both cases, so that the correction need not be made and we may take $\tau_n \cong 4/\lambda_{HH}$. Since the minimum values of the rate constant occur in this voltage region,

the minima for the two different cases can be compared directly. This comparison is shown in Table II, and provides further evidence that the voltage-dependent component of conductance is the same as the voltage-dependent potassium conductance for an unperfused axon in ASW.

Thus, there is good reason to identify the nonlinear process in the squid axon in isosmotic potassium with the potassium "n" process known for the squid axon in ASW. But what is the linear component of current? For the axon in ASW, Hodgkin and Huxley (20) found a small linear component of current which they call "leakage." Table I shows that, in most cases studied, the linear component of conductance, g_o, is approximately equal to the ASW leakage, shown in the table as g_L. There are several exceptions in the table, but in view of the poorly understood nature of leakage, we did not try to study

TABLE II

COMPARISON OF MINIMUM RATE CONSTANT FOR TRANSIENT POTASSIUM CURRENTS IN ASW AND ISOSMOTIC KCl (PERFUSED)

	Measured λ (Rate constant for n^4)	$\lambda/4$ (Rate constant for n)	Temperature	$\lambda/4$ corrected to 6°C
			°C	
No internal perfusion, external ASW (reference 20)	1.3 $msec^{-1}$	0.33 $msec^{-1}$	20	0.057 $msec^{-1}$
Internal KF, external KCl	0.492 $msec^{-1}$	0.123 $msec^{-1}$	12.5	0.056 $msec^{-1}$

these exceptions in detail. However, it seems reasonable to identify g_o as the leakage current. Furthermore, the table shows that this leakage component does not vary much with changing external potassium concentration, and that it is increased by lowering the divalent ion concentration. These two observations are in agreement with the work of Adelman and Taylor (21) on ASW leakage.

We have shown how the currents observed for perfused axons in isosmotic potassium can be related to the "n^4" and leakage currents of unperfused axons in ASW. Two other effects on the potassium currents of unperfused axons in ASW should be considered, the shift of the conductance curve along the voltage axis when Ca^{++} concentration is varied and the long time-constant potassium inactivation process.

Frankenhaeuser and Hodgkin (11) have suggested that the potassium conductance-voltage curve shifts along the voltage axis when the external calcium concentration is changed. A shift of the negative resistance region with change in external calcium concentration does indeed occur (18). However, the

diminution of the negative resistance bump for the perfused axon cannot be explained by such a shift alone.

Ehrenstein and Gilbert (2) have observed a voltage-dependent slow potassium inactivation for the unperfused squid axon. We have observed qualitatively similar effects in the perfused squid axon. This effect may cause our current-voltage curves to be slightly in error, but as indicated in reference 2, these errors are quite small as long as the large hyperpolarizing pulses are the last ones measured.

In terms of the foregoing analysis, the divalent cations have two effects on the potassium current in the perfused squid axon: they are necessary for the negative resistance, and they decrease the leakage.

We wish to thank Drs. E. Rojas and D. L. Gilbert for their participation during the early stages of this experiment, and for many helpful discussions.

We would also like to thank Dr. F. Huneeus-Cox for his demonstration of the details of his perfusion method, and Dr. M. Berman for the use of his computer program, SAAM, which we used for a least-squares fit of some of the transient data, and Dr. K. S. Cole for his helpful comments on the manuscript.

Received for publication 11 November 1966.

REFERENCES

1. MOORE, J. W. 1959. Excitation of the squid axon membrane in isosmotic potassium chloride. *Nature.* **183**:265.
2. EHRENSTEIN, G., and D. L. GILBERT. 1966. Slow changes of potassium permeability in the squid giant axon. *Biophys. J.* **6**:553.
3. SEGAL, J. R. 1958. An anodal threshold phenomenon in the squid giant axon. *Nature.* **182**:1370.
4. STÄMPFLI, R. 1958. Die Strom-Spannungs-Charakteristik der erregbaren Membran eines einzelnen Schnürrings und ihre Abhängigkeit von der Ionenkonzentration. *Helv. Physiol. Pharmacol. Acta.* **16**:127.
5. NAKAMURA, Y., S. NAKAJIMA, and H. GRUNDFEST. 1965. Analysis of spike electrogenesis and depolarizing K inactivation in electroplaques. *J. Gen. Physiol.* **49**: 321.
6. MUELLER, P., and D. O. RUDIN. 1963. Induced excitability in reconstituted cell membrane structure. *J. Theoret. Biol.* **4**:268.
7. MEISSNER, H. P. 1965. Das Verhalten der Schnürringmembran unter dem Einfluss starker Ströme. *Arch. Ges. Physiol.* **283**:213.
8. LINDEMANN, B. 1965. Negative slope Na-conductance in the surface structure of frog skin epithelium. *Biol. Bull.* **129**:391.
9. ROJAS, E., and G. EHRENSTEIN. 1965. Voltage clamp experiments on axons with potassium as the only internal and external cation. *J. Cellular Comp. Physiol.* **66** (Suppl. 2):71.
10. STEINBACH, H. B., S. SPIEGELMAN, and N. KAWATA. 1944. The effects of potassium and calcium on the electrical properties of squid axons. *J. Cellular Comp. Physiol.* **24**:147.

11. FRANKENHAEUSER, B., and A. L. HODGKIN. 1957. The action of calcium on the electrical properties of squid axons. *J. Physiol.*, (*London*). **137**:218.
12. TASAKI, I. 1963. Permeability of squid axon membrane to various ions. *J. Gen. Physiol.* **46**:755.
13. TASAKI, I., and T. TAKENAKA. 1963. Resting and action potential of squid giant axons intracellularly perfused with sodium-rich solutions. *Proc. Natl. Acad. Sci. U.S.* **50**:619.
14. OIKAWA, T., C. S. SPYROPOULOS, I. TASAKI, and T. TEORELL. 1961. Methods. for perfusing the giant axons of *Loligo pealii*. *Acta Physiol. Scand.* **52**:195.
15. MOORE, J. W., and K. S. COLE. 1963. Voltage clamp techniques. *In* Physical Techniques in Biological Research. Vol. 6, Electrophysiological Methods B. W. L. Nastuk, editor. Academic Press, Inc., New York. 263.
16. ARMSTRONG, C. M., and L. BINSTOCK. 1964. The effects of several alcohols on the properties of the squid giant axon. *J. Gen. Physiol.* **48**:265.
17. COLE, K. S. 1949. Dynamic electrical characteristics of the squid axon membrane. *Arch. Sci. Physiol.* **3**:253.
18. GILBERT, D. L. and G. EHRENSTEIN. 1965. Effect of calcium and magnesium on voltage-clamped squid axons immersed in isosmotic potassium chloride. Abstracts. 23rd International Congress Physiological Society, Tokyo. 86.
19. HODGKIN, A. L. and A. F. Huxley. 1952. A quantitative description of membrane current and its application to conduction and excitation in nerve. *J. Physiol.*, (*London*). **117**:500.
20. HODGKIN, A. L., and A. F. HUXLEY. 1952. The components of membrane conductance in the giant axon of *Loligo*. *J. Physiol.*, (*London*). **116**:473.
21. ADELMAN, W. J., and R. E. TAYLOR. 1961. Leakage current rectification in the squid giant axon. *Nature*. **190**:883.